



Papers published in *Hydrology and Earth System Sciences Discussions* are under open-access review for the journal *Hydrology and Earth System Sciences*

Surface soil moisture
estimates from
AMSR-E
observations

L. Wang et al.

Surface soil moisture estimates from AMSR-E observations over an arid area, Northwest China

L. Wang¹, J. Wen¹, T. Zhang¹, Y. Zhao², H. Tian¹, X. Shi¹, X. Wang¹, R. Liu¹,
J. Zhang¹, and S. Lu¹

¹Key Laboratory for Climate-Environment and Disasters of Western China, Cold and Arid Regions Environmental and Engineering Research Institute, Chinese Academy of Sciences, Lanzhou, Gansu 730000, China

²Xinjiang Climate Center, Urumqi, Xinjiang 830002, China

Received: 24 December 2008 – Accepted: 20 January 2009 – Published: 24 February 2009

Correspondence to: J. Wen, jwen@lzb.ac.cn

Published by Copernicus Publications on behalf of the European Geosciences Union.

Title Page

Abstract

Introduction

Conclusions

References

Tables

Figures

◀

▶

◀

▶

Back

Close

Full Screen / Esc

Printer-friendly Version

Interactive Discussion

Abstract

In this paper, 7 years (during the growing season (April–October) of 2002–2008) of the Advanced Microwave Scanning Radiometer (AMSR-E) data taken at a frequency of 6.9 GHz for night observations at both polarizations are processed and used to conduct 7 years of surface soil moisture dataset for an arid area, in Northwestern China. This soil moisture dataset can contribute to better understanding the climate change and forecast modeling for this area. Based on the first-order radiative transfer model calculation, a unique method for estimating surface soil moisture over the study area is developed. Considering extremely complex topography over the study area, we have to present a parameterization of surface roughness at the 6.9 GHz and spatial resolution of the AMSR-E using the annual minimum *MPDI* (Microwave Polarization Difference Index). For validation purpose, the comparisons of soil moisture patterns with precipitation fields are made. The results indicate the evolutions of soil moisture estimated from the AMSR-E and antecedent ground daily precipitations are in a good agreement. Furthermore, a series of rainfall traces is captured over the Taklimakan Desert. Comparisons of the estimated values of soil moisture with the ground observations are also made for two representative sites over 2002–2004. The results indicate there has a good agreement between them, with higher correlation coefficients ($R=0.649, 0.604$) and RMSE (3.5, 5.4%), and the soil moisture product derived from the AMSR-E is realistic and acceptable. This new long time series of estimated soil moisture will prove valuable for other studies of climate change and model evaluation.

1 Introduction

Surface soil moisture is a key variable of water and energy exchanges at the land surface/atmosphere interface and thus has potential applications in hydrology, meteorology, and climate change studies. For climate applications, soil moisture is considered as the most important indicator of the effect of increase in greenhouse gases on the

Surface soil moisture estimates from AMSR-E observations

L. Wang et al.

[Title Page](#)

[Abstract](#)

[Introduction](#)

[Conclusions](#)

[References](#)

[Tables](#)

[Figures](#)

◀

▶

◀

▶

[Back](#)

[Close](#)

[Full Screen / Esc](#)

[Printer-friendly Version](#)

[Interactive Discussion](#)

climate (Rowntree and Bolton, 1983). Real-time soil moisture measurements are vital for crop monitoring and drought warning. Previous researches have shown that passive microwave remote sensing sensors can be used to monitor soil moisture over land surfaces (Choudhury and Gorus, 1988; Paloscia et al., 1993; Drusch et al., 2001; Jackson, 1993; Lakshmi et al., 1997; Njoku et al., 2005; Owe et al., 2007). Investigations have established the fundamentals of passive microwave remote sensing for monitoring temporal and spatial variations of regional soil moisture (Kerr and Njoku, 1990; Mo et al., 1982). Ground-based soil moisture network can not be built reasonably without consideration of huge cost. However, satellite observations are available in real-time and provide good temporal and spatial coverage. The effects of vegetation cover and surface roughness play a significant role in the microwave emission from the surface. Therefore, good parameterization schemes of these two effects are prerequisite for retrieving surface soil moisture information. Low frequencies are preferable for soil moisture estimates since perturbing factors such as atmospheric moisture, vegetation canopy, and surface roughness are less significant. Consequently, recent advances in science and technology have resulted in space agency commitments to L-band (1.4 GHz) missions in the near future (Kerr, 2001; Kerr et al., 2007). At present, there are several new satellite sensors operating at somewhat higher frequencies than L-band that show promise for soil moisture mapping under some conditions. The Advanced Microwave Scanning Radiometer (AMSR-E) is one of them which has potential for estimating surface soil moisture in regions with low level of vegetation. In the current investigation, an alternative retrieval technique utilizing the AMSR-E 6.9 GHz observations and based upon the work of Njoku and Li (2003) is implemented and tested for an arid area.

Some typical techniques available for the estimation of surface soil moisture from the passive microwave observations are given below.

Surface soil moisture estimates from AMSR-E observations

L. Wang et al.

[Title Page](#)

[Abstract](#)

[Introduction](#)

[Conclusions](#)

[References](#)

[Tables](#)

[Figures](#)

◀

▶

◀

▶

[Back](#)

[Close](#)

[Full Screen / Esc](#)

[Printer-friendly Version](#)

[Interactive Discussion](#)



1.1 Single channel algorithm

Several significant examples of this algorithm have been performed by Jackson et al. (Jackson et al., 1995, 1999; Jackson and Le Vine, 1996), which are based on the radiative transfer equation and use a channel that is most sensitive to soil moisture.

5 This algorithm incorporates soil texture, surface roughness and temperature using h -polarized brightness temperature and also includes correction for vegetation, and is then used with a dielectric model to obtain the soil moisture.

1.2 Multichannel iterative algorithm

This approach is successfully used for AMSR-E estimates to carry out three parameters simultaneously: surface soil moisture, soil temperature and vegetation water content

10 (Njoku and Li, 1999; Njoku et al., 2003). However, unanticipated radio frequency interference (RFI) problem is encountered at the 6.9 GHz frequency (Njoku et al., 2005; Li et al., 2004), requiring modification of this approach. A radiative transfer model, the $\omega-\tau$ model, is used for this algorithm. First, the higher frequencies in terms of 18 and 37 GHz are used for surface classification. Next, the $\omega-\tau$ model is employed in comparing with the measured and the computed brightness temperatures at four channels (6.9 and 10.7 GHz, dual polarization). Finally, the three parameters are obtained until the difference between the computed and the observed brightness temperatures is minimized in a least squares sense. The principal of this algorithm is to discriminate 15 between the three parameters considering the sensitivity differences between horizontal (H) and vertical (V) polarizations, and between frequencies.

20

1.3 Polarization index algorithm

Owe et al. (2007) has shown the potential of this algorithm for developing a historical climatology of continuous satellite-derived global land surface soil moisture. The Microwave Polarization Difference Index (*MPDI*) can effectively eliminate or minimize the

Surface soil moisture estimates from AMSR-E observations

L. Wang et al.

[Title Page](#)

[Abstract](#)

[Introduction](#)

[Conclusions](#)

[References](#)

[Tables](#)

[Figures](#)

◀

▶

[Back](#)

[Close](#)

[Full Screen / Esc](#)

[Printer-friendly Version](#)

[Interactive Discussion](#)

effects of surface temperature. This algorithm uses a nonlinear iterative procedure in a forward modeling approach to separate the surface emission from the vegetation emission, and then optimizes on the vegetation optical depth and the soil dielectric constant. Once convergence between the computed and the observed brightness temperatures is achieved, the model uses a global database of soil physical properties together with a soil dielectric mixing model to solve for the surface soil moisture.

Arid and semi-arid land accounts for 40% of the earth's surface. From climatological, ecological and anthropogenic perspectives, the spatio-temporal distributions of soil moisture over arid and semi-arid land are very important. Nowadays, climate change in arid areas is one of the main focuses in global warming which the international community is most concerned about. Desertification and arid ecosystem deterioration induced by arid climate variation and their impacts on the natural environment and anthropogenic activities have been given priority in recent years.

The objective of this study is to develop a specialized model for monitoring soil moisture suitable for an arid region in Northwestern China, Xinjiang. Our research into microwave land surface soil moisture for the study area here has been motivated by a need to better understanding the climate change and forecast modeling for this area. The study area is also interesting because of diversity of its surface types and complexity of its topography. So far, no such attempt has been made exclusively for this region from literatures.

2 Study area and data descriptions

The Xinjiang Uygur Autonomous Region of China is located in the hinterland of the Eurasian continent. Lying in Northwestern China (Fig. 1), Xinjiang covers a huge area of 1 660 000 km² with 49.5% mountains, 28% plains and 22.5% deserts, occupying one-sixth of China's total territorial area and larger than any other Chinese province or autonomous region.

The Xinjiang region is characterized by its unique topography with an extremely large

Surface soil moisture estimates from AMSR-E observations

L. Wang et al.

[Title Page](#)

[Abstract](#)

[Introduction](#)

[Conclusions](#)

[References](#)

[Tables](#)

[Figures](#)

◀

▶

◀

▶

[Back](#)

[Close](#)

[Full Screen / Esc](#)

[Printer-friendly Version](#)

[Interactive Discussion](#)



elevation range from -154 m in the Turfan Basin to 8611 m at the summit of Qiaogeli. The Altay and Kunlun Mountain ranges lie in the north and the south of Xinjiang, respectively. The magnificent Tianshan Mountain, with an elevation of 3000 to 5000 m, stretches from east to west in the middle of the region, dividing Xinjiang into north and south sections. The Junggar Basin between the Tianshan and the Altay ranges contains the Gurbantunggut Desert in the middle. The Tarim Basin is enclosed by the Tianshan and the Kunlun ranges with the Taklimakan Desert in the middle.

Due to its unique geography, this area has a conspicuous continental arid climate, with large diurnal temperature range, abundant sunshine, very large potential evaporation and low precipitation. It has annual average temperatures of 4.1 – 7.8°C and 10.2 – 12.3°C for the north and the south of Xinjiang, respectively. The rainfall is concentrated mainly in the summer season, with annual precipitation of about 146 mm.

In this paper, the AMSR-E brightness temperature (TB) observations are employed for estimating soil moisture. The AMSR-E instruments onboard the EOS/Aqua platform have been a component of the Defense Meteorological Satellite Program since June, 2002. The AMSR-E instruments are a conical scanning total power microwave radiometer system operating at a constant incidence angle of 54.8° across a 1445 -km swath at six frequencies: 6.9 , 10.7 , 18.7 , 23.8 , 36.5 , and 89 GHz. All the channels operate in both V and H polarization. Spatial resolution ranges from approximately 60 km at 6.9 GHz to 5 km at 89 GHz. The orbital period is about 102 min, which results in 14.1 orbits per day. For a given satellite, coverage is possible twice a day approximately 12 h apart on the ascending and descending passes. The orbit is sun-synchronous with equator crossings at about $01:30$ and $13:30$ LT. Additional information can be found in Njoku et al. (2003).

The AMSR-E measurements used here are AMSR-E/Aqua Daily Girded Brightness Temperatures available at the National Snow and Ice Data Center (NSIDC) (Knowles 2006). They are in the north EASE-Grid projection, with all channels having 25 km resolution and equidistant latitude-longitude projection at 0.25° resolution.

The 2002–2008 daily rain-gauge data from 95 metrological stations operating in Xin-

Surface soil moisture estimates from AMSR-E observations

L. Wang et al.

[Title Page](#)

[Abstract](#)

[Introduction](#)

[Conclusions](#)

[References](#)

[Tables](#)

[Figures](#)

◀

▶

◀

▶

[Back](#)

[Close](#)

[Full Screen / Esc](#)

[Printer-friendly Version](#)

[Interactive Discussion](#)

jiang are used for validations. The data are available from the Xinjiang Climate Center of China. The stations, however, are most installed in the well-populated zones on the front plains of the mountains and the outskirts of the deserts (Fig. 1).

For further validation, we take advantage of soil moisture observations, consisting of 5 2 stations (Aletai: 88.08° E, 47.73° N and Shache: 77.27° E, 38.43° N) in the study area, for the period 2002–2004, to evaluate the estimated soil moisture from the AMSE. These observations were taken using the gravimetric technique for each 10-cm layer down to a depth of 0.5 m, The data were observed three times a month on the 8, 18 10 and 28th days, generally for the growing season (April to October). The data were originally recorded as percent wetness by mass of dry soil. Using soil density information available for each layer at each site, we determined the volumetric soil moisture. Only the data of the top layer (0–10 cm) are used for comparison purpose.

Additionally, soil moisture can not be estimated under snow cover or frozen soil conditions because the soil moisture dependence on the dielectric constant become small 15 when surface soil temperature is below 0°C (Hallikainen et al., 1985). Therefore, days with snow cover or frozen soil are eliminated from the present study. The period of the beginning of April to the end of October is, in general, historically free-frozen and snow-free for entire study area except for mountains. Thus, this period is taken into account for analysis, and hereinafter referred as to an “annual cycle”.

20 3 Theoretical background and methodology

Passive microwave remote sensing is based on the measurement of thermal radiation from the land surface in the centimeter wave band. This radiation is largely determined by two components: physical temperature and emissivity of the underlying radiating body. Many land parameters have distinct properties that affect microwave emissivity in 25 various ways. Dielectric properties and surface roughness may describe the properties.

The approach for this paper is based on the first-order radiative transfer theory. The influence of atmospheric moisture and the multiple scattering in the vegetation layer

Surface soil moisture estimates from AMSR-E observations

L. Wang et al.

[Title Page](#)

[Abstract](#)

[Introduction](#)

[Conclusions](#)

[References](#)

[Tables](#)

[Figures](#)

◀

▶

◀

▶

[Back](#)

[Close](#)

[Full Screen / Esc](#)

[Printer-friendly Version](#)

[Interactive Discussion](#)

are assumed to be neglected. Furthermore, if the soil and vegetation temperatures are approximately equal and represented by a single surface temperature T_s (K), the primary relationships between surface parameters and microwave brightness temperatures T_b can be expressed (Kerr and Wigneron, 1995; Njoku et al., 2003; Mo et al., 5 1982):

$$T_{b_p} = T_s \{e_{s_p} \Gamma_p + (1-\omega_p)(1-\Gamma_p)[1 + (1-e_{s_p})\Gamma_p]\} \quad (1)$$

where ω is single scattering albedo of the vegetation, and the subscript p is polarization of the measurement, H or V, e_s is emissivity of the soil surface which is related to the reflectivity r_{sp} by

$$10 \quad e_{s_p} = 1 - r_{s_p} \quad (2)$$

and Γ is transmissivity of the vegetation and can be expressed as a function of the vegetation opacity along the observation path:

$$\Gamma_p = \exp(-\tau_{c_p} / \cos \theta) \quad (3)$$

where θ is the incidence angle, τ_c is the vegetation opacity along the observation path 15 which could be linearly related to the total vegetation water content (VWC) using the so called b_p parameter (Jackson and Schmugge, 1991):

$$\tau_{c_p} = b_p VWC \quad (4)$$

Results of investigators have shown that the use of lower frequencies results in far less canopy attenuation of the soil emission. At lower frequencies, a value 0.15 of the 20 parameter for b is appropriate for most agriculture crops. Methods for estimating the VWC have also been developed by passive microwave remote sensing. Investigators have explored relationships between the MPDI and vegetation parameters for a given vegetation type (Paloscia et al., 2001; Wen et al., 2005; Choudhury and Tucker, 1987).

The soil reflectivity at a given incidence angle is mainly related to soil moisture 25 through the complex permittivity of the soil (Wang and Schmugge, 1980; Dobson et

Surface soil moisture estimates from AMSR-E observations

L. Wang et al.

[Title Page](#)[Abstract](#)[Introduction](#)[Conclusions](#)[References](#)[Tables](#)[Figures](#)[◀](#)[▶](#)[Back](#)[Close](#)[Full Screen / Esc](#)[Printer-friendly Version](#)[Interactive Discussion](#)

al., 1985). However, in general case, surface roughness also affects the surface reflectivity because of scattering. To account for soil roughness, the h – Q formulation (Wang et al., 1983) is often used, and then the reflectivity of a rough surface, r_{sp} , is related to that of an equivalent smooth surface, r_{op} , as follows:

$$r_{sp} = [(1 - Q)r_{op} + Qr_{oq}] \exp(-h) \quad (5)$$

where p and q denote orthogonal polarizations. The surface roughness parameter h is proportional to the quantity $(ks)^2$, where k is the wave number ($k=2\pi/\lambda$) and s is standard deviation of the surface height (cm). The parameter Q contains information on both the vertical and the horizontal roughness correlation length, l .

10 Since there are no data available to quantify the regional variability of h and Q at the AMSR-E frequencies and footprint scales, we calibrate h and Q empirically as discussed below.

15 In general, it is impossible to separate the integral contributions of surface roughness and vegetation layer unless one of them is known a priori. Investigators usually use a fixed value for roughness parameterization and assume the remainder of roughness can be automatically coupled with the vegetation effects (Owe et al., 2001; Njoku et al., 2003; Owe et al., 2007).

20 In this study, we use a numerical solution for the vegetation optical depth rather than use ancillary data or other surrogates (e.g. *NDVI*, *LAI*, and *MPDI*). The optical depth is directly derived from the *MPDI* and the dielectric constant of the soil, which improves the accuracy and overall efficiency of the soil moisture estimates. From Meesters et al. (2005), the numerical solution for the vegetation optical depth is:

$$\tau = \cos \theta \ln(ad + \sqrt{(ad)^2 + a + 1}) \quad (6)$$

25 Then, according to Eq. (3)

$$\Gamma = \frac{1}{ad + \sqrt{(ad)^2 + a + 1}} \quad (7)$$

[Title Page](#)

[Abstract](#)

[Introduction](#)

[Conclusions](#)

[References](#)

[Tables](#)

[Figures](#)

◀

▶

◀

▶

[Back](#)

[Close](#)

[Full Screen / Esc](#)

[Printer-friendly Version](#)

[Interactive Discussion](#)

where a and d are defined as

$$a = 0.5 \left(\frac{e_V - e_H}{MPDI} - e_V - e_H \right) \quad (8)$$

and

$$d = \frac{\omega}{2(1 - \omega)} \quad (9)$$

5 The *MPDI* is defined as:

$$MPDI = \frac{T_{bV} - T_{bH}}{T_{bV} + T_{bH}} \quad (10)$$

The *MPDI* is frequently used to minimize or eliminate the effects of variable surface temperature dependence, leading to a close relationship to the dielectric properties of the emitting surfaces. The *MPDI* decreases with increasing vegetation water content

10 because denser vegetation usually depolarizes the soil emission. For bare soil, the *MPDI* decreases with decreasing soil moisture because the soil emission is less polarized when the free water content in the soil is reduced.

The assumption that the vegetation single scattering has minimal effect on emissivity is widely accepted (Jackson et al., 1982). For simplicity, we neglect the effect of the 15 single scattering, and then rewrite (1) by Eq. (5)–(10) as:

$$MPDI = \frac{e_V - e_H}{e_V + e_H} (1 - 2Q) \left\{ 1 + \frac{2}{e_V + e_H} [\exp(2\tau + h) - 1] \right\}^{-1} \quad (11)$$

This equation can be reworked to the expression of the combined surface parameters of the surface roughness and the vegetation opacity, using Eq. (5) :

$$\tau + 2h = \cos \theta \ln[0.5 * (1 - 2Q)(r_{Ho} - r_{Vo})MPDI^{-1} + r_{Ho} + r_{Vo}] \quad (12)$$

20 In Eq. (11), there are three parameters unknown: the two parameters of surface roughness and the soil moisture that affects the soil emissivity. It is evident that if the

Surface soil moisture estimates from AMSR-E observations

L. Wang et al.

[Title Page](#)

[Abstract](#)

[Introduction](#)

[Conclusions](#)

[References](#)

[Tables](#)

[Figures](#)

◀

▶

◀

▶

Back

Close

[Full Screen / Esc](#)

[Printer-friendly Version](#)

[Interactive Discussion](#)



values of surface roughness corresponding to Q and h are available, we can readily estimate the soil temperature. However, the ancillary data of surface roughness are sparse. For lower frequency (at 1.4 GHz), Q would have a minimum effect on the surface moisture calculations, while h also is usually used with a lower value. Therefore, 5 when surface roughness conditions may be unknown, a value of zero is often assigned to Q , and a value between 0 and 0.3 is typically assumed for h (Jackson, 1993). At the 6.9 GHz frequency, Njoku and Chan (2006) used Q as a fixed global calibration factor leaving h to incorporate the roughness spatial variability. For the desert region in Saudi Arabia, with a global minimal topographic variation, a value of Q (0.174) was adopted 10 as a fixed parameter to calibrate the AMSR-E data globally to the microwave model for a baseline minimum roughness level, assuming $h=0$.

The challenge for us is to separate these variables from the emitting signal by using a minimum of ancillary data. Apart from the brightness temperature data, we have only the ancillary data of soil texture. As previously mentioned, the study area is characterized 15 by its extremely complex topography. Assuming the value of Q assigned as 0.174, if the value of h is assigned a fixed value (e.g., 0.2), the soil moisture estimates could not be made for many places of this study area except for desert regions. The reason for this explanation is that the value of h is uniform and probably much higher for the regions of complex topography. We have therefore realized using a uniform value of h 20 for entire area is not reasonable. For clarity, the theoretical relationship between the *MPDI* and the vegetation optical depth is simulated with the radiative equation (Eq. 10) before solving for this issue using a more unique approach (Fig. 2).

For bare soil, Fig. 2a shows the *MPDI* increases nonlinearly with increasing soil moisture, while for vegetated soil *MPDI* has a more complex relationship to soil moisture. 25 The two effects of soil moisture and vegetation water content on the *MPDI* are synergistic in general. *MPDI* decreases when vegetation water content increases and/or soil moisture decreases. When vegetation water content increases the *MPDI* sensitivity to soil moisture decreases rapidly. Additionally, when *MPDI* is less than 0.01 or the vegetation optical depth is approximately greater than 0.8, the information

Surface soil moisture estimates from AMSR-E observations

L. Wang et al.

[Title Page](#)

[Abstract](#)

[Introduction](#)

[Conclusions](#)

[References](#)

[Tables](#)

[Figures](#)

◀

▶

◀

▶

[Back](#)

[Close](#)

[Full Screen / Esc](#)

[Printer-friendly Version](#)

[Interactive Discussion](#)

of soil moisture is attenuated by high vegetation biomass and therefore can not be derived. Additionally, Fig. 2b depicts the relationship between the *MPDI* and the vegetation optical depth for a range of surface roughness ($k=12$). The two effects of surface roughness and vegetation water content on the *MPDI* are also interactive. It can be seen that sensitivity of the *MPDI* to soil moisture decreases nonlinearly very rapidly with surface roughness. This nonlinear attenuation effect of surface roughness is very similar to that of vegetation water content. Therefore, some investigators combined the two effects into one parameter to conduct temporal dynamics of vegetation water content (Njoku and Chan, 2006) and surface soil moisture (Jin and Yan, 2007).

As there are minimal human activities in the study area, the roughness is practically less disturbed for the AMSR-E footprint size. Once the roughness is estimated carefully, it may remain fairly invariable with time. First, we assumed the roughness is unchanging during an annual cycle. We further supposed the dries soil to have ~5.5% volumetric soil moisture. The later assumption was probably somewhat higher for desert regions while lower for other regions. Note that the penetration depth at 6.9 GHz is only approximately 1.0–2.0 cm (Jackson and Schmugge, 1989). There are no soil moisture measurements in this depth, although, it is self-evident that the soil moisture at this depth is in general lower than that at deeper depth (e.g. 5 cm). Njoku et al. (2006) speculated the value of volumetric soil moisture (VSM) in dry soil condition in the desert region of Al-Hadidah is round 5.0%.

For bare surface, the minimal VSM corresponds to the minimal *MPDI* ($MPDI_{min}$) from the AMSR-E observed over an annual cycle. The threshold for distinguishing between vegetated and bare soil surfaces using the *MPDI* is about 0.04 at 6.9 GHz (Wang et al., 2006). We assumed the values of the VSM for the driest bare soil in this study area are slight higher than that in region of Al-Hadidah, thus 5.5% was a reasonable value of VSM in dries surface soil condition. This baseline minimum value was used ultimately to compute h at each footprint for bare soil ($MPDI_{min} > 0.04$). As a consequence, total footprints for bare soil account for 62.3% in this study area. The others involved vegetated soil, frozen soil, snow cover, glacier etc. Figure 3 is the map

Surface soil moisture estimates from AMSR-E observations

L. Wang et al.

[Title Page](#)

[Abstract](#)

[Introduction](#)

[Conclusions](#)

[References](#)

[Tables](#)

[Figures](#)

◀

▶

[Back](#)

[Close](#)

[Full Screen / Esc](#)

[Printer-friendly Version](#)

[Interactive Discussion](#)

of the $MPDI_{min}$ for 2005, clearly distinguishing the bare soils from other surface types. Ignoring a very few abnormal negative values, the areas corresponding to the $MPDI_{min}$ not greater than 0.01 are just the glaciers lying on the mountains of Tianshan, Altay and Kunlun mountain each. The areas corresponding to the $MPDI_{min}$ ranging from 0.01 to 0.02 are usually characterized by perennial snow covers on mountains or some dense forests. As for the areas corresponding to the $MPDI_{min}$ ranging from 0.02 to 0.04, they indicate the ever presence of vegetation. Note throughout this paper that the areas ranging from 0.02 to 0.04 only indicate that there were covered by vegetations all the time or just at times. That is to say, there were less vegetations or bare soils covering the same areas at some or even long time for a given annual cycle.

Figure 4 shows the map of the h parameter in 2005 over the study area derived by Eq. (12). All the h patterns for other years are almost the same as this one. Note that the lower values of h correspond to the areas of dry, flat, and comparably homogeneous soil conditions, especially the Taklimakan Desert and the Gurbantunggut Desert.

The maximum value of h in bare soil areas is 0.73 and higher values of h mostly exists in the transition zones between deserts and mountains (purple color) where are characterized by great gradients of DEM. Considering the continuity of the h distribution and that the non-bare areas are mostly related to steep mountains, we predisposed empirically the value of the h parameter as 0.6.

20 4 Algorithm implementation, results and validations

4.1 Implementation

The previously described methodology has been applied to the historical dataset of nighttime AMSR-E brightness temperatures for the study area. A 7-year time series of estimated daily soil moisture dataset was obtained. Considering the greater stability of nighttime surface temperatures, only nighttime data were used in the study. Additionally, days with snow cover or frozen soil were also eliminated from the analysis, and

Surface soil moisture estimates from AMSR-E observations

L. Wang et al.

[Title Page](#)

[Abstract](#)

[Introduction](#)

[Conclusions](#)

[References](#)

[Tables](#)

[Figures](#)

◀

▶

◀

▶

[Back](#)

[Close](#)

[Full Screen / Esc](#)

[Printer-friendly Version](#)

[Interactive Discussion](#)

therefore we just have selected the growing season (April to October).

An iterative procedure was developed for the forward radiative transfer model that iteratively computed the simulated *MPDI* for VSM ranging from 5.5% to 45%, in 0.1% increments. The single-scattering albedo of the vegetation was set as 0.0 for both H and V polarization. At each iteration step, for 6.9 GHz, the computed *MPDI* values were compared to the satellite observations. If the absolute value of the differences between the computed and observed *MPDI* was less than 0.0015, then the input soil moisture would be saved in array. During the iteration process, the dielectric mixing model developed by Hallikainen et al. (1985) was used to convert VSM into soil dielectric constant. This mixing model requires percent of sand and clay as input, in addition to VSM. The soil texture classification of the surface soil on a 1-km grid for this study area was used here (Webb et al., 1991). For each AMSR-E footprint the soil texture properties were retrieved.

4.2 Results

15 4.2.1 Mean annual soil moisture patterns

Figure 5 depicts the 7-year estimated mean annual soil moisture patterns. These patterns are similar to each other. In general, the mean annual soil moisture is around 9%. The lower values exist in desert regions especially in the Taklimakan Desert, and higher values are present on Northeastern Kunlun Mountain and in the transition zones between deserts and mountains, where are drainage regions. Significantly, the glaciers and/or snow covers distributed on the tops of mountains are automatically computed as no-value regions where the convergence between the calculated and the observed *MPDI* was no longer achieved because of the extremely low *MPDI* resulting from depolarization prosperities of glaciers and snow covers.

25 In order to further explore the dynamic characteristics of soil moisture, the year 2005 was selected for this investigation.

Surface soil moisture estimates from AMSR-E observations

L. Wang et al.

[Title Page](#)

[Abstract](#)

[Introduction](#)

[Conclusions](#)

[References](#)

[Tables](#)

[Figures](#)

◀

▶

◀

▶

[Back](#)

[Close](#)

[Full Screen / Esc](#)

[Printer-friendly Version](#)

[Interactive Discussion](#)

4.2.2 Annual maximum soil moisture pattern

HESSD

6, 1055–1087, 2009

Surface soil moisture estimates from AMSR-E observations

L. Wang et al.

[Title Page](#)

[Abstract](#)

[Introduction](#)

[Conclusions](#)

[References](#)

[Tables](#)

[Figures](#)

◀

▶

◀

▶

[Back](#)

[Close](#)

[Full Screen / Esc](#)

[Printer-friendly Version](#)

[Interactive Discussion](#)



For each of the locations, matches between estimated soil moistures and antecedent measured daily precipitations were made. Furthermore, we selected typical a series of rainfall events in 2005 for regional validation. Finally, we compared the AMSR-E estimates of VSM and ground observations for two reprehensive sites, the Aletai site and Shache site, on the 8, 18 and 28th days over 2002–2004.

5 4.3.1 Temporal variability of estimated soil moisture

Six stations were selected as the representatives for different surface types (vegetated surface, desert surface, bare arid surface) and climatic characteristics (the north and the south climate, separately). Figure 7 shows time series of estimated VSM and antecedent observed precipitation in 2005 for six representative locations – Tazhong (83.67° E, 90.00° N), Qinghe (90.38° E, 46.67° N), Shache (77.27° E, 38.43° N), Yutian (81.65° E, 36.85° N), Hetian (79.93° E, 36.85° N), and Mosuowan (86.10° E, 45.02° N). In general, the temporal patterns of precipitation and soil moisture for both bare and vegetated soil condition are characteristically coincident. The first three locations represent bare soil condition, particularly Tazhong just lies in the center of the Taklimakan Desert. The others represent vegetated soil condition. It can be seen that Tazhong is mostly associated with extremely low soil moisture condition (5.5% VSM) except for the rainy days when soil moisture increases up sensitively and afterwards decreases to original lever quickly. This must be a result of very high evaporative demand in this region. Qinghe and Shache show the characteristic behavior of soil moisture where it also increases up responding to rainfall event evidently. In addition, high dispersions of soil moisture are observed for these two locations. Highly variable surface temperature for the two locations could be responsible for this reason. On the other hand, Yutian, Hetian, and Mosuowan show lower dispersions compared to locations of bare soil, although soil moisture also responses to rainfall event evidently. However, after rainfall event, soil moisture gradually decreases. This lag is largely attributed to the retention capacity of soli moisture of vegetated soil.

Surface soil moisture
estimates from
AMSR-E
observations

L. Wang et al.

[Title Page](#)

[Abstract](#)

[Introduction](#)

[Conclusions](#)

[References](#)

[Tables](#)

[Figures](#)

◀

▶

[Back](#)

[Close](#)

[Full Screen / Esc](#)

[Printer-friendly Version](#)

[Interactive Discussion](#)

4.3.2 Regional distributions of estimated soil moisture

To broaden validating the soil moisture dataset, regional validation was conducted using precipitation observations over the study area. There are comparatively sparse meteorological stations in the huge area, although, a series of typical rainfall events was found. The events occurred on 4–6 August 2005 (DOY of 216–218), which were characterized in the IR images by a long belt of frontal cloud crossing the study area from north to south. High estimated soil moisture conditions were captured during the rainfall period. The frontal system traveled the Taklimakan Desert from west to east, producing light to moderate rainfall. Dry conditions (10% VSM) prevailed at the beginning of the rainfall events over the Taklimakan Desert. During the rainfall period, the Taklimakan Desert shows a series of rainfall traces with three sequential center regions of increased soil moisture conditions. The maximum values of estimated soil moisture reaches 22.0%, 29.2% and 37.8% for these three center regions, respectively. Note that the soil moisture conditions in these regions became rapidly dry after these meteorological events.

4.3.3 Comparison with in situ observations

Validation of the soil moisture retrieval algorithm here is based on comparisons of the AMSR-E estimates of VSM and ground observations for two sites, the Aletai site and Shache site, on the 8, 18 and 28th days over 2002–2004. Figure 9 shows comparisons of the measured soil moisture with the estimated soil moisture for the two sites. Generally, the estimated soil moisture has temporal scale comparable to observations, but has small amplitude of variation. This small amplitude can be attributed to low sensitivity of soil moisture at FOV scale compared to that at point scale. In spite of some dispersion in data, higher correlation coefficients ($R=0.649$, 0.604 for the two sites, respectively) and RMSE (3.5, 5.4%) are shown in Table 1. we can conclude that the algorithm is quite able to estimate the correct value of VSM. Figure 10 shows plots of estimated verse measured soil moisture for the two sites. Generally, the algorithm

Surface soil moisture estimates from AMSR-E observations

L. Wang et al.

[Title Page](#)

[Abstract](#)

[Introduction](#)

[Conclusions](#)

[References](#)

[Tables](#)

[Figures](#)

◀

▶

◀

▶

[Back](#)

[Close](#)

[Full Screen / Esc](#)

[Printer-friendly Version](#)

[Interactive Discussion](#)

overestimates the soil moisture amount on the dry condition (below 14%) and, on the contrary, underestimates the soil moisture amount on the wet condition (above 14%), with positive average differences on the order of 2%.

These results clearly demonstrate that the estimated VSM from the AMSR-E is consistent with the ground observations, which strongly supports the developed retrieval algorithm.

5 Conclusion and discussions

A model for estimating surface soil moisture over the arid area of Xinjiang, Northwest China, from the AMSR-E brightness temperatures at 6.9 GHz was developed. This

model was based on first-order radiative transfer model calculation and applied to conduct 7-year period (2002–2008) of soil moisture dataset. Finally, we compared the estimated soil moisture with the measured precipitation. Results clearly demonstrated the performance of the model for soil moisture estimates in the study area. The temporal patterns of rainfall and soil moisture for both bare and vegetated soil condition were characteristically coincident and soil moisture also responded to rainfall event evidently, especially for bare soil condition. Furthermore, we captured a series of rainfall traces over the Taklimakan Desert. To quantitatively analyse the accuracy of the product derived from the AMSR-E, comparisons of the estimated soil moisture with the ground observations were also made for two representative sites. The results indicated the estimated soil moisture followed well these ground observations at temporal scale. Moreover, higher correlation coefficients ($R=0.649, 0.604$) were obtained, indicating there has a good agreement between them and the soil moisture product derived from the AMSR-E is realistic and acceptable.

Two important model parameters were calibrated a priori. One was vegetation optical depth which was calibrated using an excellent numerical solution which made it possible to separate the effects of surface roughness and vegetation, especially over bare soil regions. The other was surface roughness which was fine-tuned with elab-

Surface soil moisture estimates from AMSR-E observations

L. Wang et al.

[Title Page](#)

[Abstract](#)

[Introduction](#)

[Conclusions](#)

[References](#)

[Tables](#)

[Figures](#)

◀

▶

◀

▶

[Back](#)

[Close](#)

[Full Screen / Esc](#)

[Printer-friendly Version](#)

[Interactive Discussion](#)

orate assumptions for bare soil and vegetated soil, respectively. The later is worth further discussing as follows.

Surface roughness parameterization is needed prior to surface soil moisture estimates, particularly in complex topographic region. We have supposed the soil moisture corresponds 5.5% for the dries bare soil. Additionally, for vegetated soil, we empirically assigned the parameter h with a uniform value 0.6. These assumptions allow possible and even reliable h parameterization, which has not been possible until now in this study area. However, these guesses would be not right for some footprints. On the other hand, the previous assumption of a value of zero for the single scattering for various vegetations is also unrealistic. In practice, to some extent, the higher assigned h value can offset the effect of underestimation of the single scattering, and then improve the quality of soil moisture estimates.

In addition, the assumed minimum value of 5.5% VSM, for example, must be some higher for some desert soils. ~3% may be a realistic guess. However, this input could lead to a negative h value. Volume scattering can account for this issue. This uncertainty in the h parameterization will propagate into the retrieval algorithm as part of the soil moisture biases, although, the present study shows progress in the characterization of the surface roughness, and proves potential for surface moisture estimates.

Moreover, the model is mathematically well behaved, so convergence is normally fast and the glaciers and/or snow covers distributed on the tops of mountains can be computed as no-value regions automatically. The estimated soil moisture dataset now has been made available for climate analysis and forecast modeling for the study area.

References

Choudhury, B. J. and Tucker, C. J.: Monitoring global vegetation using Nimbus-7 37 GHz Data Some empirical relations, *Int. J. Remote Sens.*, 8, 1085–1090, 1987.

Choudhury, B. J. and Golus, R.: Estimating soil wetness using satellite data, *Int. J. Remote Sens.*, 9, 1251–1257, 1988.

Surface soil moisture estimates from AMSR-E observations

L. Wang et al.

[Title Page](#)

[Abstract](#)

[Introduction](#)

[Conclusions](#)

[References](#)

[Tables](#)

[Figures](#)

◀

▶

◀

▶

[Back](#)

[Close](#)

[Full Screen / Esc](#)

[Printer-friendly Version](#)

[Interactive Discussion](#)



5 Dobson, M., Ulaby, F., Hallikainen, M., and El-Rayes, M.: Microwave Dielectric Behavior of Wet Soil-Part II: Dielectric Mixing Models, *IEEE T. Geosci. Remote Sens.*, 23, 35–46, 1985.

Drusch, M., Wood, E., and Jackson, T.: Vegetative and Atmospheric Corrections for the Soil Moisture Retrieval from Passive Microwave Remote Sensing Data: Results from the Southern Great Plains Hydrology Experiment 1997, *J. Hydrometeorol.*, 2, 181–192, 2001.

10 Hallikainen, M. T., Ulaby, F. T., Dobson, M. C., and El-Rayes, M. A.: Microwave Dielectric Behavior of Wet Soil-Part 1: Empirical Models and Experimental Observations, *IEEE T. Geosci. Remote Sens.*, 23, 25–34, 1985.

Jackson, T., Schmugge, T., and Wang, J.: Passive Microwave Sensing of Soil Moisture Under Vegetation Canopies, *Water Resour. Res.*, 18, 1137–1142, 1982.

15 Jackson, T. and Schmugge, T.: Passive microwave remote sensing system for soil moisture: some supporting research, T. *IEEE Geosc. Remote Sens.*, 27, 225–235, 1989.

Jackson, T. and Schmugge, T.: Vegetation effects on the microwave emission of soils, *Remote Sens. Environ.*, 36, 203–212, 1991.

20 Jackson, T.: Measuring surface soil moisture using passive microwave remote sensing, *Hydrol. Proc.*, 7, 139–152, 1993.

Jackson, T., Le Vine, D., Swift, C., Schmugge, T., and Schiebe, F.: Large area mapping of soil moisture using the ESTAR passive microwave radiometer in Washita'92, *Remote Sens. Environ.*, 54, 27–37, 1995.

25 Jackson, T. and Le Vine, D.: Mapping surface soil moisture using an aircraft-based passive microwave instrument: algorithm and example, *J. Hydrol.*, 184, 85–99, 1996.

Jackson, T., Le Vine, D., Hsu, A., Oldak, A., Starks, P., Swift, C., Isham, J., and Haken, M.: Soil moisture mapping at regional scales using microwaveradiometry: the Southern Great Plains Hydrology Experiment, *IEEE T. Geosci. Remote Sens.*, 37, 2136–2151, 1999.

30 Jin, Y. and Yan, F.: A change detection algorithm for terrain surface moisture mapping based on multi-year passive microwave remote sensing (Examples of SSM/I and TMI Channels), *Hydrol. Proc.*, 21, 1918–1924, 2007.

Kerr, Y. H. and Njoku, E. G.: A semiempirical model for interpreting microwave emission from semiarid land surfaces as seen from space, *IEEE T. Geosci. Remote Sens.*, 28, 384–393, 1990.

Kerr, Y. H. and Wigneron, J. P.: Vegetation models and observations – A review, in: *Passive Microwave Remote Sensing of Land-Atmosphere Interactions*, edited by: Pampaloni, B. T. C., Kerr, Y. H., and Njoku, E. G., VSP, The Netherlands, 28, 317–344, 1995.

Surface soil moisture estimates from AMSR-E observations

L. Wang et al.

[Title Page](#)

[Abstract](#)

[Introduction](#)

[Conclusions](#)

[References](#)

[Tables](#)

[Figures](#)

◀

▶

[Back](#)

[Close](#)

[Full Screen / Esc](#)

[Printer-friendly Version](#)

[Interactive Discussion](#)



Kerr, Y. H., Waldteufel, P., Wigneron, J. P., Martinuzzi, J., Font, J., and Berger, M.: Soil moisture retrieval from space: the Soil Moisture and OceanSalinity (SMOS) mission, *IEEE T. Geosci. Remote Sens.*, 39, 1729–1735, 2001.

Kerr, Y. H.: Soil moisture from space: Where are we?, *Hydrogeol. J.*, 15, 117–120, 2007.

5 Knowles, K. W., Savoie, M. H., Armstrong, and Brodzik, M. J.: updated current year. AMSR-E/Aqua daily EASE-Grid brightness temperatures, 2005. Boulder, Colorado, USA: National Snow and Ice Data Center, Digital media, 2006

Lakshmi, V., Wood, E., and Choudhury, B.: Evaluation of Special Sensor Microwave/Imager Satellite Data for Regional Soil Moisture Estimation over the Red River Basin, *J. Appl. Meteorol.*, 36, 1309–1328, 1997.

10 Li, L., Njoku, E., Im, E., Chang, P., and Germain, K.: A preliminary survey of radio-frequency interference over the US in Aqua AMSR-E data, *IEEE T. Geosci. Remote Sens.*, 42, 380–390, 2004.

Meesters, A., De Jeu, R., and Owe, M.: Analytical derivation of the vegetation optical depth from the microwave polarization difference index, *IEEE Geosci. Remote Sens. Lett.*, 2, 121–123, 2005.

15 Mo, T., Choudhury, B. J., Schmugge, T. J., and Jackson, T. J.: A model for microwave emission from vegetation-covered fields, *J. Geophys. Res.*, 87, 1229–1237, 1982.

Njoku, E. G., and Li, L.: Retrieval of land surface parameters using passive microwave measurements at 6–18 GHz, *IEEE T. Geosci. Remote Sens.*, 37, 79–93, 1999.

20 Njoku, E. G., Jackson, T. J., Lakshmi, V., Chan, T. K., and Nghiem, S. V.: Soil moisture retrieval from AMSR-E, *IEEE T. Geosci. Remote Sens.*, 41, 215–229, 2003.

Njoku, E. G., Ashcroft, P., and Chan, T. K.: Global survey and statistics of radio-frequency interference in AMSR-E land observations, *IEEE T. Geosci. Remote Sens.*, 43, 938–947, 2005.

25 Njoku, E. and Chan, S.: Vegetation and surface roughness effects on AMSR-E land observations, *Remote Sens. Environ.*, 100, 190–199, 2006.

Owe, M., de Jeu, R., Walker, J., Branch, H. S., Center, N., and Greenbelt, M. D.: A methodology for surface soil moisture and vegetation opticaldepth retrieval using the microwave polarization difference index, *IEEE T. Geosci. Remote Sens.*, 39, 1643–1654, 2001.

30 Owe, M., de Jeu, R., and Holmes, T.: Multi-Sensor Historical Climatology of Satellite-Derived Global Land Surface Moisture, *J. Geophys. Res.*, 113, F01002, doi:10.1029/2007JF000769, 2008.

Surface soil moisture estimates from AMSR-E observations

L. Wang et al.

[Title Page](#)

[Abstract](#)

[Introduction](#)

[Conclusions](#)

[References](#)

[Tables](#)

[Figures](#)

[◀](#)

[▶](#)

[Back](#)

[Close](#)

[Full Screen / Esc](#)

[Printer-friendly Version](#)

[Interactive Discussion](#)



Paloscia, S., Pampaloni, P., Chiarantini, L., Coppo, P., Gagliani, S., and Luzi, G.: Multifrequency passive microwave remote sensing of soil moisture and roughness, *Int. J. Remote Sens.*, 14, 467–483, 1993.

Paloscia, S., Macelloni, G., Santi, E., and Koike, T.: A multifrequency algorithm for the retrieval of soil moisture on a large scale using microwave data from SMMR and SSM/I satellites, *IEEE T. Geosci. Remote Sens.*, 39, 1655–1661, 2001.

Rowntree, P. R. and Bolton, J. A.: Simulation of the atmospheric response to soil moisture anomalies over Europe, *Q. J. Roy. Meteor. Soc.*, 109, 501–526 1983.

Wang, J. and Schmugge, T.: An Empirical Model for the Complex Dielectric Permittivity of Soils as a Function of Water Content, *IEEE T. Geosci. Remote Sens.*, 18, 288–295, 1980.

Wang, J., O'Neill, P., Jackson, T., and Engman, E.: Multifrequency Measurements of the Effects of Soil Moisture, Soil Texture, And Surface Roughness, *IEEE T. Geosci. Remote Sens.*, 21, 44–51, 1983.

Wang, L., Li, Z., and Quan, C.: Soil moisture retrieval with AMSR-E in the region with vegetation coverage, *High Tech. Lett.*, 16, 204–209, 2006. (In Chinese)

Webb, R., Rosenzweig, C., Levine, E., Aeronautics, U. S. N., Scientific, S. A., and Program, T. I.: A Global Data set of Soil Particle Size Properties, National Aeronautics and Space Administration, Office of Management, Scientific and Technical Information Program, online available at: <http://www.daac.ornl.gov> (last access: 2 November 2008), 1991.

Wen, J., Jackson, T., Bindlish, R., Hsu, A., and Su, Z.: Retrieval of Soil Moisture and Vegetation Water Content Using SSM/I Data over a Corn and Soybean Region, *J. Hydrometeorol.*, 6, 854–863, 2005.

Surface soil moisture estimates from AMSR-E observations

L. Wang et al.

[Title Page](#)

[Abstract](#)

[Introduction](#)

[Conclusions](#)

[References](#)

[Tables](#)

[Figures](#)

◀

▶

◀

▶

[Back](#)

[Close](#)

[Full Screen / Esc](#)

[Printer-friendly Version](#)

[Interactive Discussion](#)

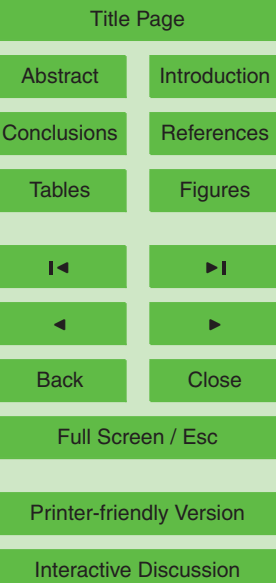


Surface soil moisture
estimates from
AMSR-E
observations

L. Wang et al.

Table 1. Statistics of estimated and measured VSM for the Shache site and the Aletai site over 2002–2004.

Site	Mean of Estimated VSM	Mean of Measured VSM	Difference	Standard Deviation of Difference	RMSE	Correlation Coefficient Between Estimated and Measured VSM	Record Number
(%)							
Shache	10.1	8.3	1.8	3.02	3.5	0.649	37
Aletai	11.5	9.3	2.2	2.79	5.4	0.604	48



Surface soil moisture estimates from AMSR-E observations

L. Wang et al.

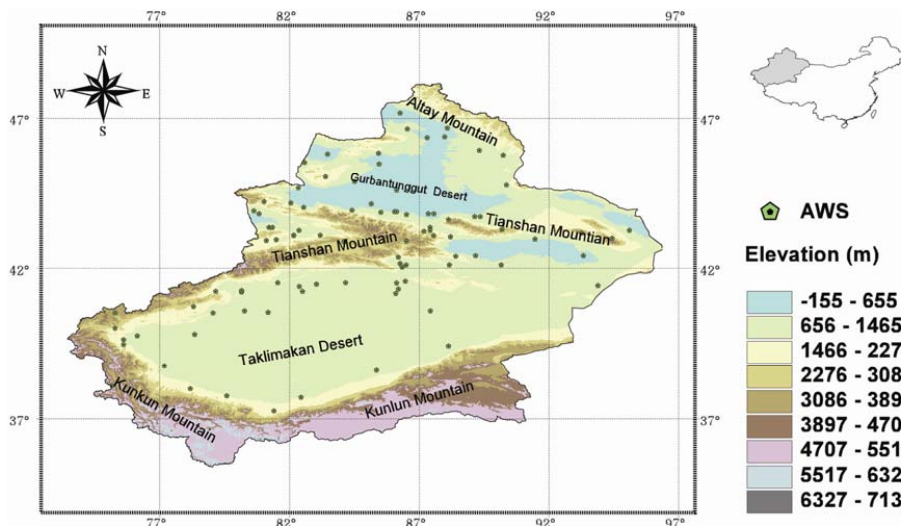


Fig. 1. Map of the study area combined with digital elevation model (DEM) and distribution of the meteorological observation network.

- [Title Page](#)
- [Abstract](#) [Introduction](#)
- [Conclusions](#) [References](#)
- [Tables](#) [Figures](#)
- [◀](#) [▶](#)
- [◀](#) [▶](#)
- [Back](#) [Close](#)
- [Full Screen / Esc](#)
- [Printer-friendly Version](#)
- [Interactive Discussion](#)

Surface soil moisture estimates from AMSR-E observations

L. Wang et al.

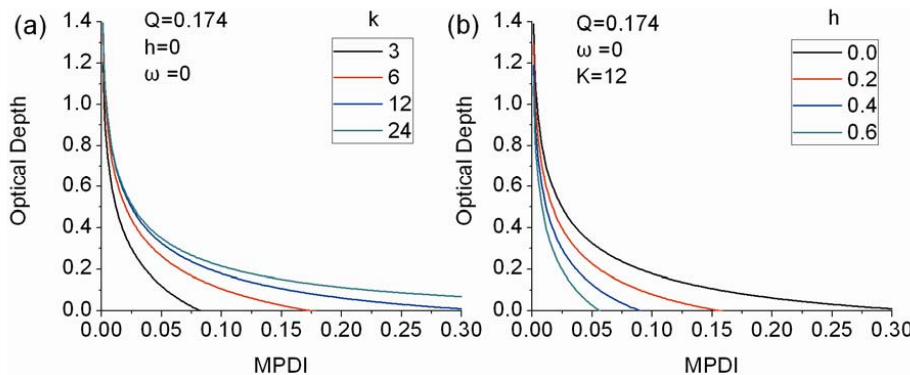


Fig. 2. Theoretical relationship between the *MPDI* and the vegetation optical depth, **(a)** a range of soil dielectric constants ($Q=0.174$, $h=0$, and $\omega=0$), **(b)** surface roughness ($Q=0.174$, $h=0$, and $k=12$).

- [Title Page](#)
- [Abstract](#) [Introduction](#)
- [Conclusions](#) [References](#)
- [Tables](#) [Figures](#)
- [◀](#) [▶](#)
- [◀](#) [▶](#)
- [Back](#) [Close](#)
- [Full Screen / Esc](#)
- [Printer-friendly Version](#)
- [Interactive Discussion](#)

Surface soil moisture
estimates from
AMSR-E
observations

L. Wang et al.

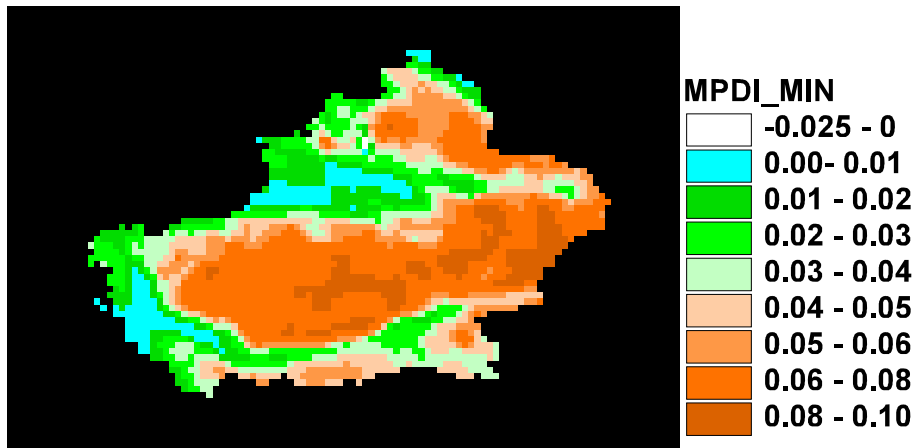


Fig. 3. Distribution of the calculated minimal *MPDI* for 2005.

- [Title Page](#)
- [Abstract](#) [Introduction](#)
- [Conclusions](#) [References](#)
- [Tables](#) [Figures](#)
- [◀](#) [▶](#)
- [◀](#) [▶](#)
- [Back](#) [Close](#)
- [Full Screen / Esc](#)
- [Printer-friendly Version](#)
- [Interactive Discussion](#)

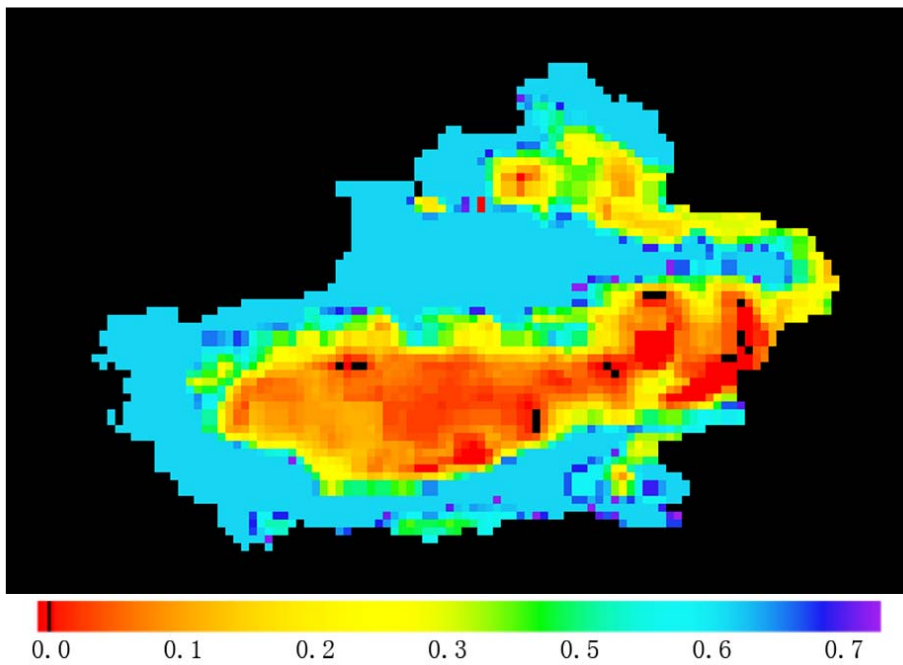


Fig. 4. Distribution of the estimated h parameter for 2005.

**Surface soil moisture
estimates from
AMSR-E
observations**

L. Wang et al.

[Title Page](#)

[Abstract](#)

[Introduction](#)

[Conclusions](#)

[References](#)

[Tables](#)

[Figures](#)

◀

▶

[Back](#)

[Close](#)

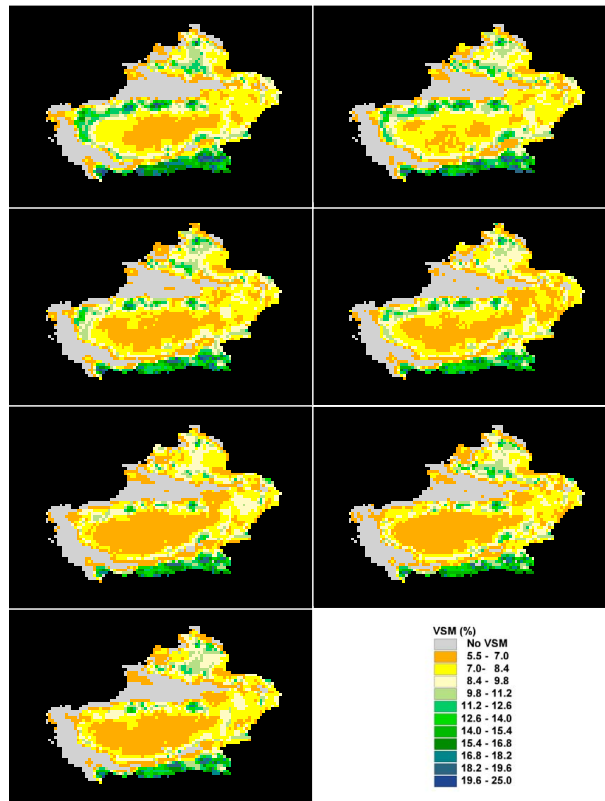
[Full Screen / Esc](#)

[Printer-friendly Version](#)

[Interactive Discussion](#)

**Surface soil moisture
estimates from
AMSR-E
observations**

L. Wang et al.



VSM (%)	
No VSM	
5.5 - 7.0	
7.0 - 8.4	
8.4 - 9.8	
9.8 - 11.2	
11.2 - 12.6	
12.6 - 14.0	
14.0 - 15.4	
15.4 - 16.8	
16.8 - 18.2	
18.2 - 19.6	
19.6 - 25.0	

Fig. 5. Patterns of mean annual surface soil moisture estimated from the AMSR-E at night orbit for years from 2002 to 2008.

[Title Page](#)

[Abstract](#)

[Introduction](#)

[Conclusions](#)

[References](#)

[Tables](#)

[Figures](#)

◀

▶

◀

▶

[Back](#)

[Close](#)

[Full Screen / Esc](#)

[Printer-friendly Version](#)

[Interactive Discussion](#)

**Surface soil moisture
estimates from
AMSR-E
observations**

L. Wang et al.

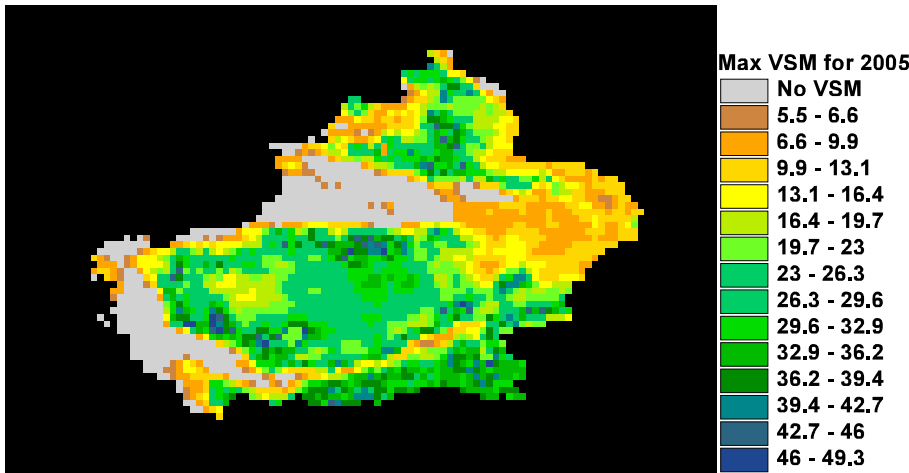


Fig. 6. Map of maximum surface soil moisture for year of 2005.

[Title Page](#)
[Abstract](#) [Introduction](#)
[Conclusions](#) [References](#)
[Tables](#) [Figures](#)

[◀](#) [▶](#)
[◀](#) [▶](#)
[Back](#) [Close](#)
[Full Screen / Esc](#)

[Printer-friendly Version](#)

[Interactive Discussion](#)

Surface soil moisture estimates from AMSR-E observations

L. Wang et al.

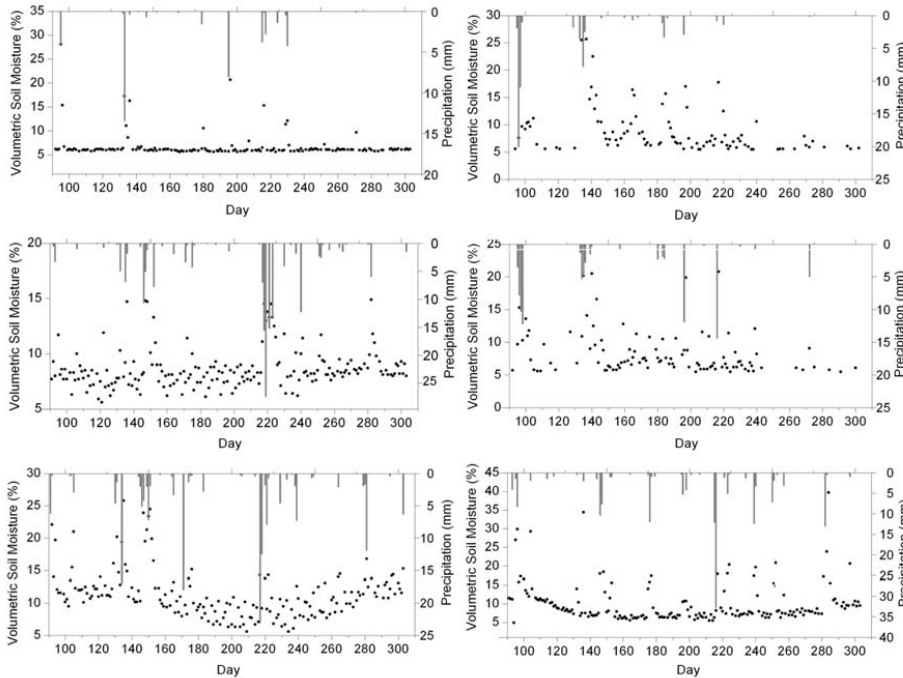


Fig. 7. Comparisons of estimated soil moisture and measured precipitation at six representative locations. Left column are representative to bare soil condition (from top to bottom, corresponding to locations Tazhong, Qinghe, Shache, and right column to vegetated soil condition for Yutian, Hetian, and Mosuowan.

- [Title Page](#)
- [Abstract](#) [Introduction](#)
- [Conclusions](#) [References](#)
- [Tables](#) [Figures](#)
- [◀](#) [▶](#)
- [◀](#) [▶](#)
- [Back](#) [Close](#)
- [Full Screen / Esc](#)
- [Printer-friendly Version](#)
- [Interactive Discussion](#)

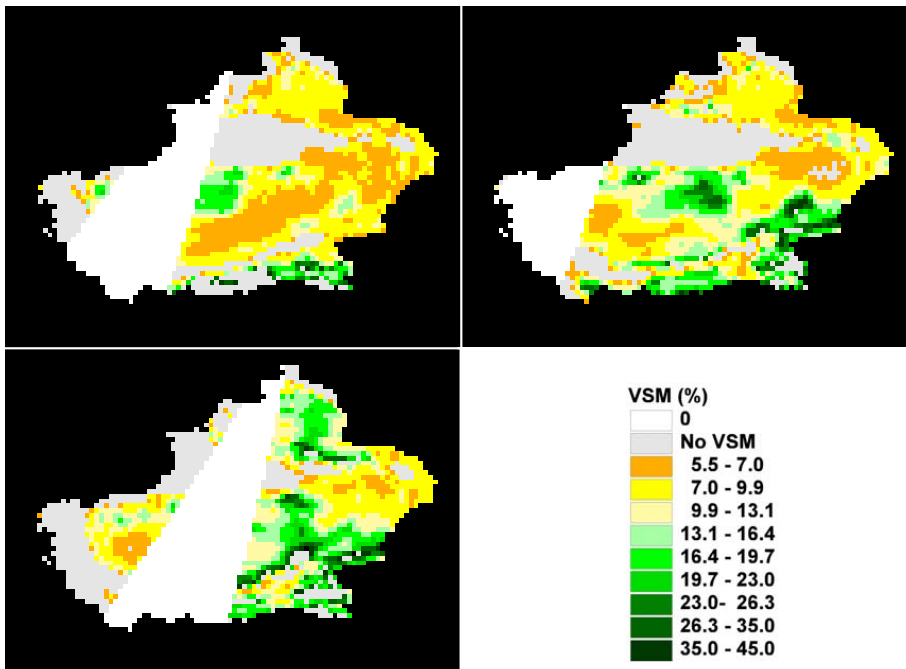


Fig. 8. Dynamics of surface soil moisture resulting from a series rainfall events during 216 to 218 of 2005.

Surface soil moisture estimates from AMSR-E observations

L. Wang et al.

[Title Page](#)

[Abstract](#)

[Introduction](#)

[Conclusions](#)

[References](#)

[Tables](#)

[Figures](#)

◀

▶

[Back](#)

[Close](#)

[Full Screen / Esc](#)

[Printer-friendly Version](#)

[Interactive Discussion](#)

Surface soil moisture estimates from AMSR-E observations

L. Wang et al.

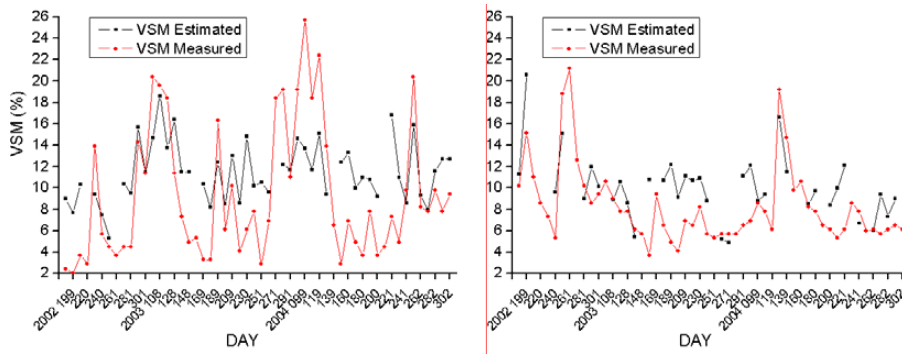


Fig. 9. Time series of estimated VSM corresponding to on the 8, 18 and 28th days (Beijing Time) for the growing season (April to October) from 189 of 2002 through 2008. Left is for the Aletai site and right is for Shache site.

- [Title Page](#)
- [Abstract](#) [Introduction](#)
- [Conclusions](#) [References](#)
- [Tables](#) [Figures](#)
- [◀](#) [▶](#)
- [◀](#) [▶](#)
- [Back](#) [Close](#)
- [Full Screen / Esc](#)

Printer-friendly Version

Interactive Discussion

Surface soil moisture estimates from AMSR-E observations

L. Wang et al.

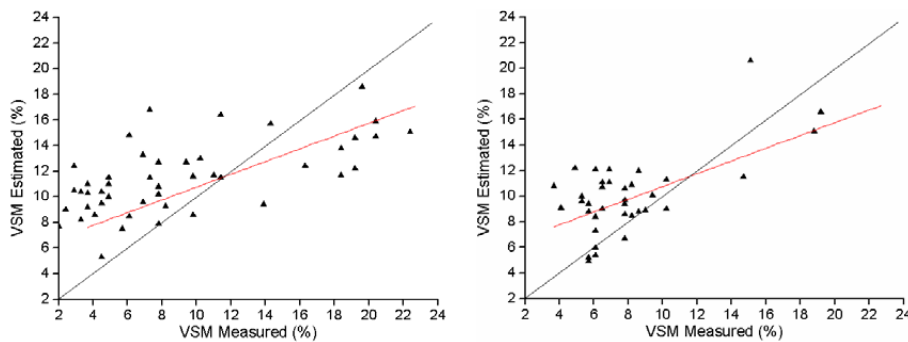


Fig. 10. Estimated VSM versus measured VSM for the Aletai site (left) and the Shache site (right) over 2002–2004. The black line represents the 1:1 line and the red one represents the fit line.

- [Title Page](#)
- [Abstract](#) [Introduction](#)
- [Conclusions](#) [References](#)
- [Tables](#) [Figures](#)
- [◀](#) [▶](#)
- [◀](#) [▶](#)
- [Back](#) [Close](#)
- [Full Screen / Esc](#)

Printer-friendly Version

Interactive Discussion